

FACTORS ACTING ON THE BOUNDARY LAYER TRANSITION  
AT HYPERSONIC SPEED

R.Michel

FACILITY FORM 602

**N67 13787**

(ACCESSION NUMBER)

15

(PAGES)

(NASA CR OR TMX OR AD NUMBER)

(THRU)

(CODE)

12

(CATEGORY)

Translation of "Facteurs agissant sur la transition de la  
couche limite aux vitesses hypersoniques".  
Office National d'Études et de Recherches Aéronautiques,  
Chatillon-sous-Bagneux. Paper No. ICAS-17, Presented at  
the Third International Congress in the Aeronautical  
Sciences, Stockholm, Sweden, August 27-31, 1962.

GPO PRICE \$ \_\_\_\_\_

CFSTI PRICE(S) \$ \_\_\_\_\_

Hard copy (HC) 1.00Microfiche (MF) 1.50

ff 653 July 65

NATIONAL AERONAUTICS AND SPACE ADMINISTRATION  
WASHINGTON OCTOBER 1966

## FACTORS ACTING ON THE BOUNDARY LAYER TRANSITION AT HYPERSONIC SPEED

R.Michel

National Aerospace Research and Development Administration,  
Chatillon-sous-Bagneux, France

Presented at the Third International Congress in the Aeronautical Sciences  
August 27-31, 1962 Stockholm, Sweden

ICAS Secretariat: IAS  
2 East 64th Street  
New York 21, N.Y.

Paper No. ICAS-17

Price:\$1.00 (U.S.)

FACTORS ACTING ON THE BOUNDARY LAYER TRANSITION  
AT HYPERSONIC SPEED

\*/1

R.Michel

Preliminary experimental results obtained in a wind tunnel at high Reynolds number and at a Mach number close to 7 are presented and discussed. By visualization and calculation of the boundary layers, the limits of the transition domain for ogives and cylinder-cone configurations of various vertex angles are determined. The variation in the nose angle and thus in the pressure gradients upstream of the body result in a considerable variation of the transition Reynolds number, based on local conditions. The length of the transition region is of the order of the laminar sector, where a considerable thickening of the boundary layer occurs. The apparent friction in the transition domain was found to be much greater than the turbulent friction.

Notations

$x$ = longitudinal coordinate, counted from the nose,	$p_{10}$ = generating stagnation pressure of the wind tunnel,
$R$ = radius of the cylindrical portion of the mockups,	$p_{11}$ = stagnation pressure downstream of the frontal shock wave,
$r$ = local radius of the ogives,	$T_{10}$ = generating temperature,
$L$ = length of the ogive portion,	$\delta$ = thickness of the boundary layer,
$\alpha_s$ = half-angle at the vertex,	$\delta_2$ = thickness of the moment of momentum,
$\varphi$ = specific mass,	$c_f$ = coefficient of friction.
$\nu$ = kinematic viscosity,	
$U_\infty, M_\infty$ = velocity and Mach number at the nose of the models,	
$U_e, M_e$ = local velocity and Mach number on the models,	

1. Introduction

/2

In this paper, we are presenting the first results of a systematic experimental study for analyzing, based on wind-tunnel tests, the principal factors that might influence the boundary layer transition, in practical problems encountered at high velocities.

The greatest of the difficulties encountered in an experimental study on the transition in a supersonic wind tunnel is no doubt the influence of the

---

\* Numbers given in the margin indicate pagination in the original foreign text.

pressure level and of the generating temperature which, all other conditions remaining constant, manifests itself in a considerable increase in the transition Reynolds number with the unit Reynolds number of the wind tunnel. A plausible explanation of the phenomenon was given in experiments by Laufer and Vrebalovich (Ref.1); these experiments showed in fact that a considerable turbulence can be spread by the turbulent boundary layers of the walls of the test section. Connected with the thickness of the boundary layer displacement, its intensity decreases with increasing unit Reynolds number. The experiments by Laufer showed also that the turbulence increases rapidly with the Mach number.

Thus, for making a valid analysis of the transition and the factors influencing it, the wind-tunnel tests must be made at unit Reynolds numbers that will be higher the greater the Mach number. This reasoning had induced us, in an earlier investigation at a Mach number of 3, to use a high pressure wind tunnel (Ref.2). For the research described here, scheduled at a Mach number of 7, we required the special arrangement of an extreme-pressure wind tunnel, with a pressure as high as 200 atm.

The results, just as those given by Michel (Ref.2), thus have the interesting feature of having been obtained at unit Reynolds numbers far superior to those mentioned in any previously published papers. As a typical example, the present conditions and those obtained earlier (Ref.2) are plotted in Fig.1 with respect to the conditions used in a rather important study by Potter and Whitfield (Ref.3); these agree fairly well with the values of the unit Reynolds numbers most often encountered in data published on the transition at various Mach numbers.

As reported previously (Ref.2), the experimental program covered the influence of pressure gradients and of the geometric form for bodies of revolution. The research covered an experimental determination of the transition region for ogive-cylindrical bodies of a previously investigated family (Ref.2). For <sup>/3</sup> comparison purposes and for judging the influence of an abrupt expansion produced at the shoulder, these investigations were complemented by a study on cylinder-cone configurations having the same vertex angle as the previously investigated ogives.

The present paper comprises a description of the technique used in determining the boundaries of the transition region, a presentation and discussion of the values obtained at transition Reynolds numbers, and their comparison with the results obtained at Mach 3.

## 2. Experimental Technique

The experiment was made in an open-throat pilot tunnel at the Fluid Mechanics Laboratory of the ONERA\* at Chalais-Meudon, laid out for producing a Mach number of 7 in a circular test section of 140 mm diameter.

---

\* ONERA = Office National d'Études et de Recherches Aéronautiques; National Aerospace Research and Development Administration.

For obtaining the very high desired pressure and the required temperature at Mach 7, the compression produced by the slow displacement of a piston in a cylinder of great length, mounted in front of the collector, was used (Ref.4).

The tests were made at a pressure of 170 - 200 bars and at a temperature of 680 - 690°K. The duration of the gusts was 0.5 sec on the average, with the measurements made 0.2 sec after start-up. Under these conditions, it was possible to keep the heating of the mockups to a negligible level and to maintain the wall temperature practically equal to the ambient pressure. The ratio of the wall temperature to the generating temperature was 0.43 on the average.

An experimental assembly scheme is shown in Fig.2. An existing conical tube of 4.5° half-angle was used. The mockups, aligned along the axis of the jet, were arranged in such a fashion that the transition, in the schlieren field, took place slightly downstream of the exit plane of the duct. For each obstacle, the Mach number along the axis of the duct was designated by  $M_\infty$ , at the abscissa of the upstream leading edge.

A tabulation of the principal geometric characteristics of the investigated bodies and of the test conditions with respect to each is given in Fig.3. The study included a cone of 5° half-angle and two families of bodies of revolution with pointed nose.

The first family, studied previously (Ref.2) at Mach 3, is composed of ogive-cylindrical bodies defined by the general equation

$$\frac{r}{R} = 2 \frac{z}{L} \left[ 1 - \left( \frac{z}{L} \right)^2 + \frac{1}{2} \left( \frac{z}{L} \right)^3 \right]$$

Three different aspect ratios were used for the ogive ahead of the cylinder, which permits, by varying the nose angle and the attached shock wave, to obtain stagnation pressures and different local Mach numbers on the cylindrical section. 4

The second family is composed of three cylinder-cone configurations whose nose angles are equal to those of the preceding bodies.

For these six models, the diameter D of the cylinder is 25 mm; the mockups are made of steel.

A determination of the limits of the transition zone is essentially based on a schlieren visualization of the boundary layer. Three examples of the obtained photographs are given in Fig.4, showing that a considerable thickening of the boundary layer is produced at these Mach and Reynolds numbers. We were able to measure the thickness of the boundary layer with satisfactory accuracy. Below, we will demonstrate that a comparison of this measurement with the data calculated for the upstream laminar boundary layer and for the downstream turbulent boundary layer, has made it possible to determine the beginning and end of the region in which the boundary layer transformation takes place.

### 3. Results and Discussions

#### 3.1 Distribution of the Local Mach Number over the Bodies

Figure 5 shows the distribution of the local Mach number over the seven models. The data are obtained from a calculation, satisfactorily confirmed by some local pressure measurements and including the two following phases:

The theory of characteristics was first applied to each body in order to determine the distribution of local Mach numbers in the case of a uniform upstream flow at a Mach number  $M_\infty$  corresponding to the abscissa of the leading edge of each mockup; this was 6.75 for the ogives and the cylindrical cones and 7 for the cone itself. At this Mach number, the theory of characteristics yields a result differing little from that obtained by the shock-expansion approximation, a property which is used in the second phase of the calculation.

After this, two corrections for taking the effects of the source flow in the conical duct into consideration, were applied. The first of these refers to the velocity increase from the abscissa of the leading edge and to the corresponding increase in the Prandtl-Meyer angle along the axis of the conical duct. It has been assumed that the same increase should be applied at each point of the Prandtl-Meyer angle corresponding to the local flow about each model. The second correction refers to the directional effect of the source flow. It was again assumed here that the local Prandtl-Meyer angle was increased at each point of the model from the angle under which the point is "viewed" from the throat of the duct. /5

The distributions in Fig.5 show the general slope expected for such bodies. Intense negative pressure gradients are present on the ogival portion of the bodies of the first family, while an abrupt expansion takes place at the junction of the cylinder-cone configuration. Along the cylindrical section, the source effect of the conical duct ensures a uniformly accelerated flow. The variation in angle at the nose manifests itself here in a considerable change in the local Mach number which thus, at the beginning of the transition, covers a range extending from 4.15 to 7.30.

#### 3.2 Determination of the Limits of the Transition Region

The photographs obtained under the above conditions permitted measuring on each mockup the thickening of the boundary layer during the transition phenomenon. Figures 6 and 7, for different bodies, give the evolution, along the abscissa, of the boundary layer thickness.

The diagrams also give the thickness of the laminar boundary layer calculated from the leading edge, as well as the calculated thickness of the turbulent boundary layer which adjoins that of the observed boundary layer downstream from this point. These calculations were made in accordance with a method developed previously (Ref.5). Based on the Kármán equation, the method yields the thickness of the moment of momentum. The laminar thickness was derived from this under the hypothesis of a velocity profile transformed from the polynomial Polhausen profile of the sixth degree. In the turbulent domain, a velocity

profile in powers has been used. In these calculations, allowance has been made for the variations in local Mach number upstream of the body and along the cylindrical section.

Figures 6 and 7 show that the observed thickness is in good agreement with the calculated thickness for the laminar boundary layer up to a fairly well-defined point, which must be considered as the beginning of the transition region. The thickness calculated for the turbulent boundary layer adjoins the observed thickness after a point whose definition is less precise but which must be considered as representing the end of the transition zone.

### 3.3 Transition Reynolds Numbers

The transition data can be interpreted from the values of Reynolds numbers that can be formed either with the abscissa  $x$  or with a characteristic thickness of the boundary layer which, very generally, is the thickness of the moment of momentum. Figure 8 shows the thicknesses of the moment of momentum, calculated for the laminar boundary layer along the models and the corresponding Reynolds numbers based on the local flow.

For ogives and cylinder-cone configurations, Fig.9 gives the Reynolds numbers of the abscissa of the beginning and end of the transition, formed with the conditions corresponding, on the one hand, to the Mach number  $M_\infty$  and, on the other hand, to the local Mach number. The diagram also gives the Reynolds number of the thickness of the moment of momentum at the beginning of transition. For the cone, the corresponding values are as follows:

<u>Start of transition</u>			<u>End of transition</u>	
$\frac{U_\infty x}{Y_\infty}$	$\frac{U_e x}{Y_e}$	$\frac{U_e \delta_z}{Y_e}$	$\frac{U_\infty x}{Y_\infty}$	$\frac{U_e x}{Y_e}$
(Millions)	(Millions)		(Millions)	(Millions)
5.30	5.55	8.80	11.50	10.45

An analysis of Fig.9 shows first that high values for the transition abscissa Reynolds number are obtained when this number is based on conditions corresponding to  $M_\infty$ . The values are slightly higher than those observed (Ref.2) at Mach 3.08\*.

The transition region extends over a considerable distance, since it is always of the order of magnitude of the length of the laminar path.

Finally, the transition Reynolds numbers of the cylindrical ogives and the cylindrical cones are distinctly higher than those for the cone alone, which

---

\* The tests at Mach 3.08 were made for the case of a practically zero heat flux at the wall, whereas a negative heat flux traverses the wall in the actual tests. Nevertheless, the published results show that the influence of the heat flux on the transition must be low at the relatively high Mach numbers considered in the present case.

seems to indicate that a considerable influence of the pressure gradients on the frontal bodies exists. Slightly more advanced transitions on the cylindrical cones apparently are due to a slightly more rapid thickening of the laminar boundary layer.

The influence of the nose cone is more distinct for Reynolds numbers based on local conditions. The resultant values are that much lower than the preceding values as the angle at the leading edge is larger. The increase in aspect ratio thus manifests itself in a considerable increase in the transition Reynolds number, a phenomenon also observed at Mach 3.

The diagram referring to the Reynolds number for the thickness of the <sup>/7</sup> moment of momentum at the beginning of transition results in comparable observations. However, it will be noted that the difference between the results at  $M_\infty = 6.75$  and at  $M_\infty = 3.08$  increases with decreasing nose angle. At the same time, the difference between the local Mach numbers at which the transition takes place also increases.

### 3.4 Apparent Friction in the Transition Region

Figures 6 and 7 show that, in all cases, the thickening of the boundary layer in the transition region is so rapid that it by far exceeds that of a turbulent boundary layer. This result, valid for the thickness of the boundary layer, is most likely also true for the thickness of the moment of momentum. In fact, the theory shows that the ratio  $\delta_2/\delta$  of a laminar boundary layer, under the actual conditions, differs little from that of a turbulent boundary layer. We assume that this layer will be maintained also for a transition boundary layer.

The Kármán equation then permits a correlation of the friction coefficient at the wall with the thickness of the moment of momentum and its derivative. We thus have

$$\frac{c_f}{2} = \frac{4}{3} \frac{\delta_2}{\delta} + \frac{\delta_2}{\delta} \frac{d\delta}{dx} + \delta_2 \frac{H + 2 - H^2}{u_\infty} \frac{du_\infty}{dx}$$

Therefore, we made an estimate of the friction coefficient in the transition region, on the basis of the above formula\*. Three examples of the obtained result are plotted in Fig.10. It is obvious that the friction resulting from the Kármán equation in the transition region is distinctly greater than the turbulent friction, as could be predicted from the rapid thickening of the boundary layer.

At first glance, this effect appears to exert a considerable influence on the balance of frictional drag and probably also on the heat flux along the wall. However, it should be emphasized that the Kármán equation, obtained by integra-

---

\* Since the ratio  $H$  of the displacement thickness to the moment of momentum thickness is unknown, the term due to the exterior velocity gradient could not be allowed for; in the present case, this will be at most 20% of the total balance.

tion of the Navier-Stokes equations, also makes the hypothesis that the longitudinal variation of the turbulence terms can be neglected, a hypothesis which obviously is highly disputable in a transition region. The result of an application of the Karman equation must be considered as "apparent" friction which might possibly contain, together with the friction along the wall, a supplementary term produced by the longitudinal derivative of the turbulent intensity.

#### 4. Conclusions

/8

Experiments made in a wind tunnel at high unit Reynolds number, with various forms of bodies of revolution with pointed nose, have shown that the favorable influence of negative pressure gradients, established on the nose cones, is still great at Mach 7.

The experiments have confirmed that the transition region, at elevated Mach numbers, reaches a considerable extent which is of the order of magnitude of the extent of the laminar path.

The data also show that a considerable thickening of the boundary layer takes place during the transition. The resultant apparent friction exceeds by far that of a turbulent boundary layer.

#### REFERENCES

1. Laufer, J. and Vrebalovich, T.: Stability of a Supersonic Laminar Boundary Layer on a Flat Plate. Jet Propulsion Lab, CIT Pasadena, Report No.20-116, December 1958.
2. Michel, R.: Localization of the Transition by Perturbation of the Boundary Layer in Supersonic Regime (Localisation de la transition par perturbation de la couche limite en régime supersonique). AGARD, Rept. No.271, April 1960.
3. Potter, J.L. and Whitfield, J.D.: Effects of Unit Reynolds Number, Nose Bluntness, and Roughness on Boundary Layer Transition. AGARD, Rept. No.256, April 1960.
4. Rebuffet, P.: Research Hypersonic Wind Tunnels of the ONERA (Souffleries hypersoniques de recherches de l'ONERA). Fourth European Aeronautical Congress, Cologne, Sept. 1960, Tech. Sci. Aeron., No.3, 1961.
5. Michel, R.: Development of the Boundary Layer in a Hypersonic Duct (Développement de la couche limite dans une tuyère hypersonique). AGARD Congress, Rhode St-Genese, Belgium, April 1962.

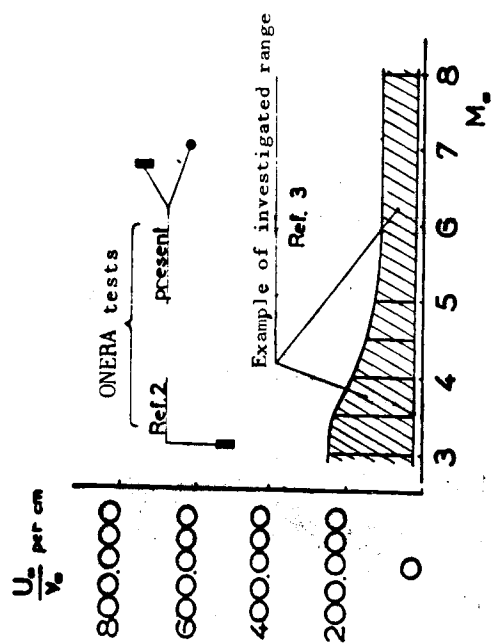


Fig.1 Unit Reynolds Numbers Involved.

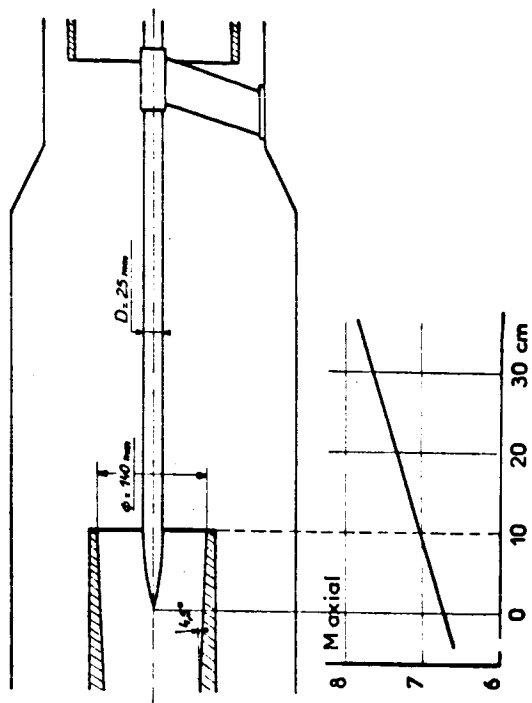


Fig.2 Sketch of Experimental Assembly.

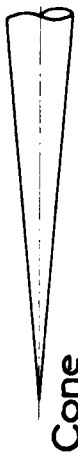


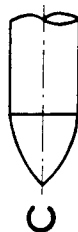
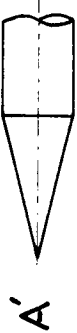
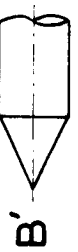
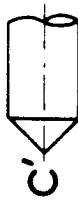
	$\frac{L}{D}$	$L$ cm	$\frac{\alpha_s}{2}$ deg.	$P_{t,0}$ bars	$P_{t,1}$ bars	$T_{t,0}$ °K	$M_\infty$
 Cone		25	5	172	171.5	680	7
 A	4	10	14.04	186.5	131.5	680	6.75
 B	2	5	26.57	196	41.6	680	6.75
 C	1	2.5	45	199	9.4	690	6.75
 A'	2	5	14.04	191	135	680	6.75
 B'	1	2.5	26.57	196	41.6	680	6.75
 C'	0.5	1.25	45	199	9.4	690	6.75

Fig.3 Bodies Investigated and Test Conditions.

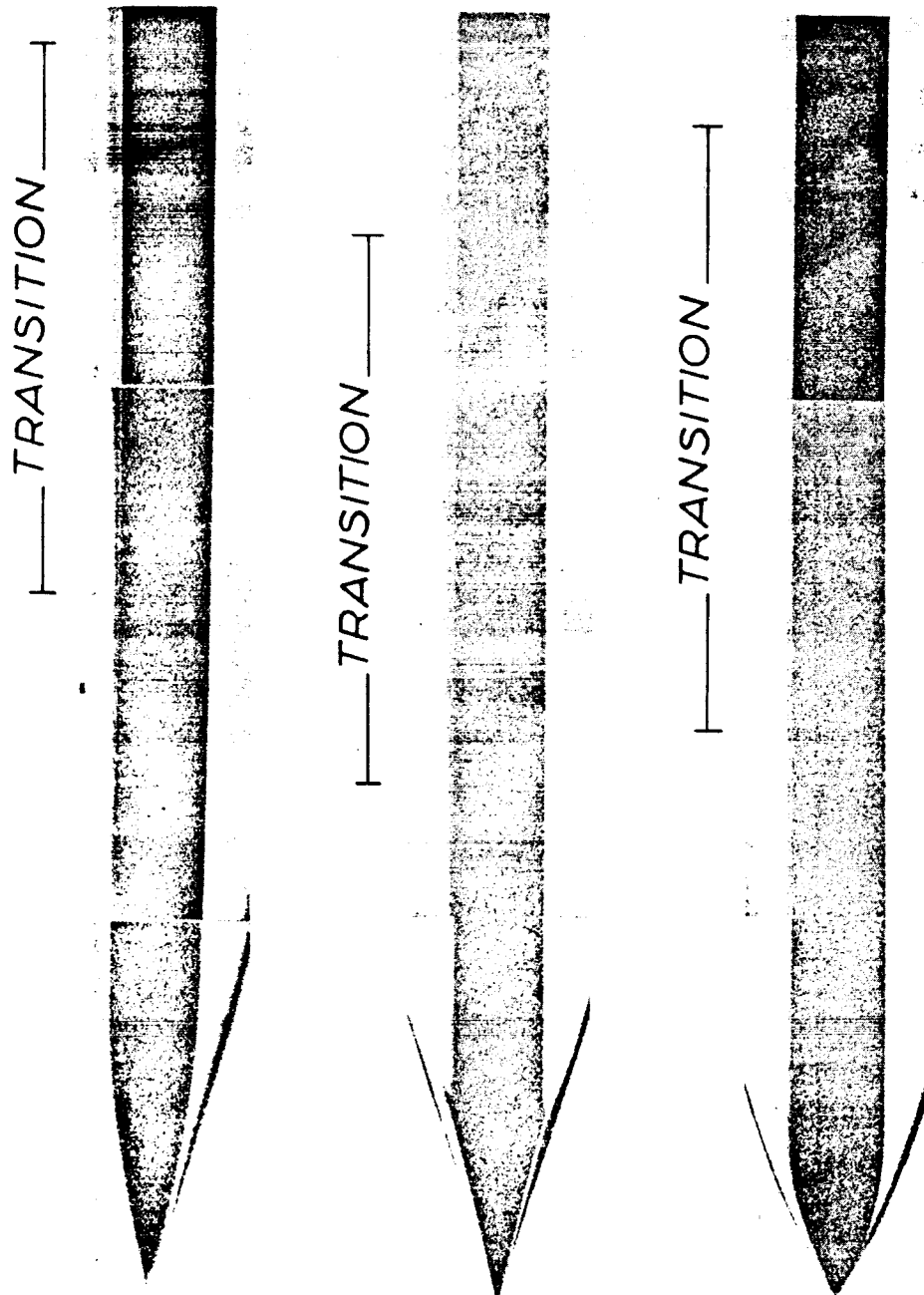


Fig.4 Examples of Schlieren Pictures of the Boundary Layer.

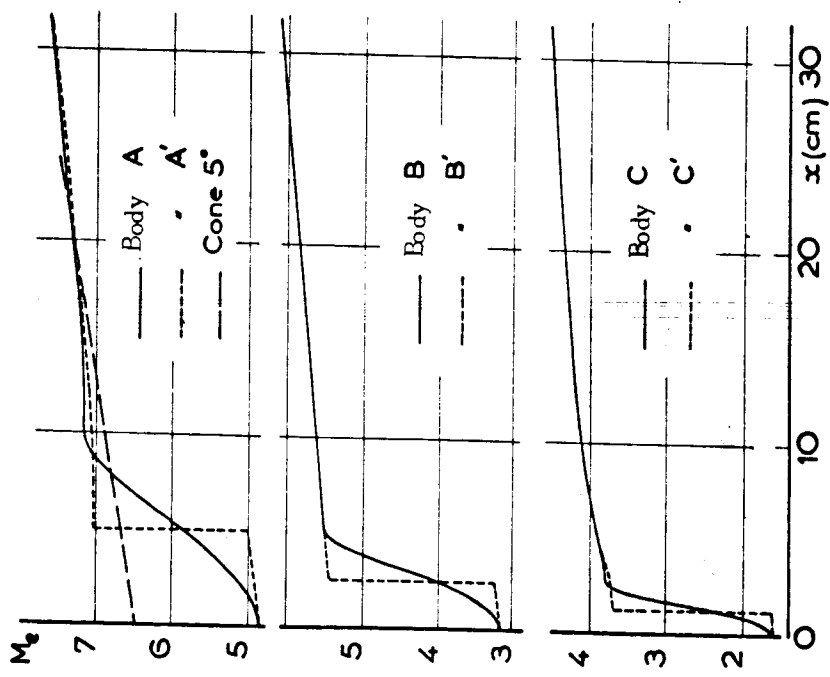


Fig.5 Distributions of the Local Mach Number.

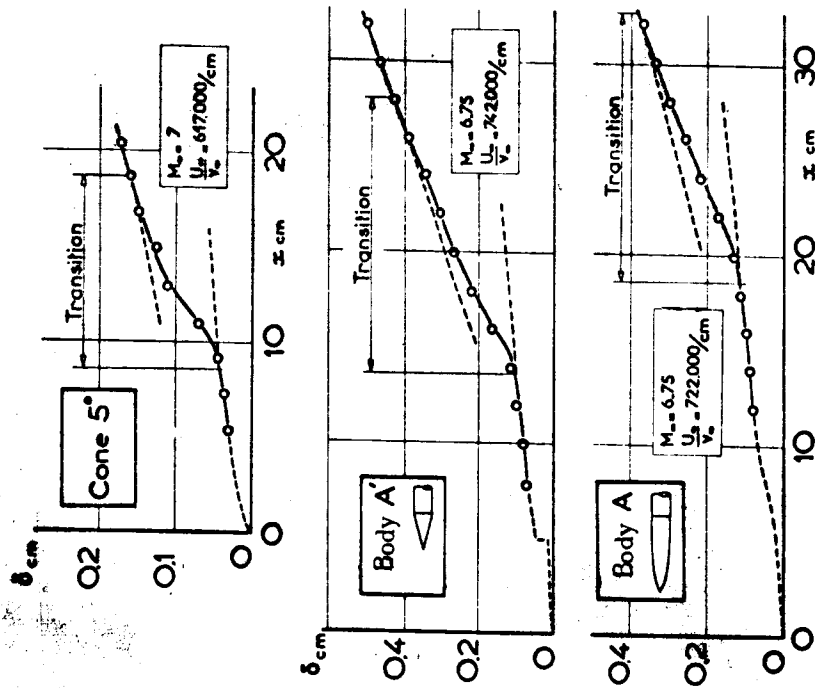


Fig.6 Thickening of the Boundary Layer and Transition - Cone, Bodies A and A' - .

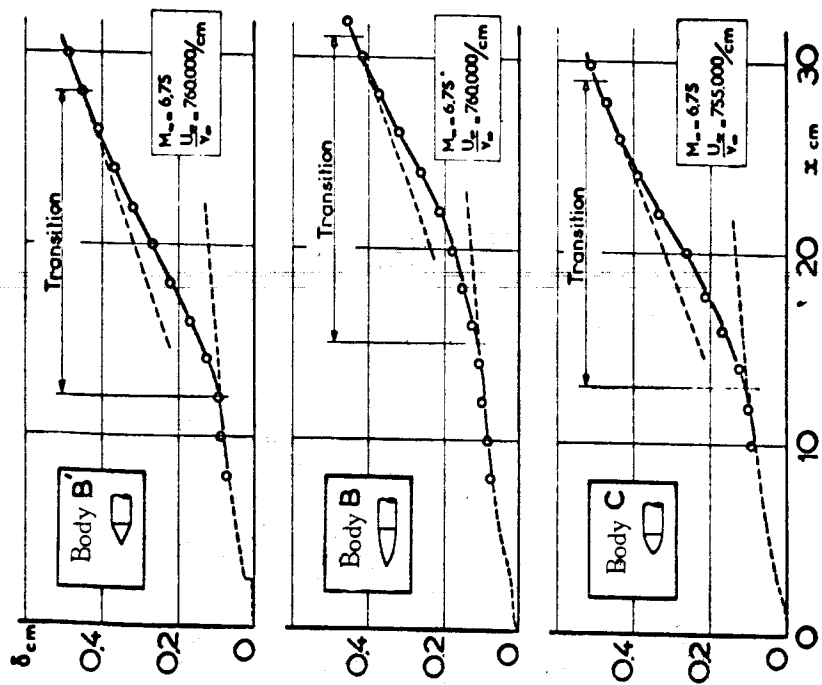


Fig.7 Thickening of the Boundary Layer and Transition - Bodies B, B', and C - -

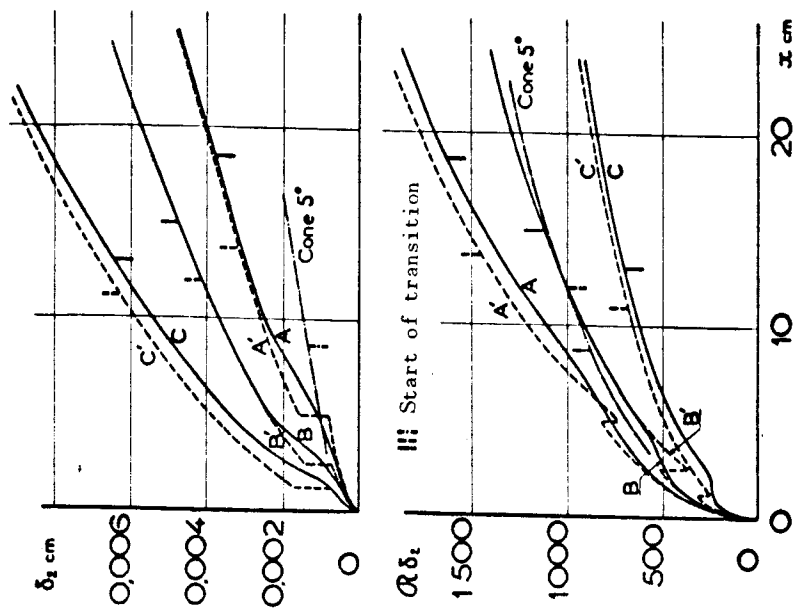


Fig.8 Thicknesses of the Laminar Moment of Momentum and Corresponding Reynolds Numbers.

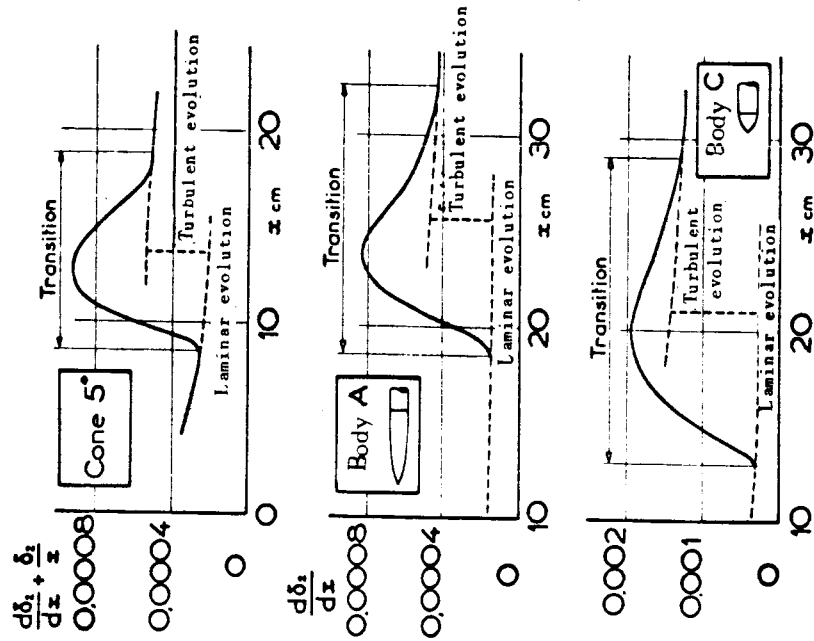


Fig.10 Principal Term of Apparent Friction in the Transition Region.

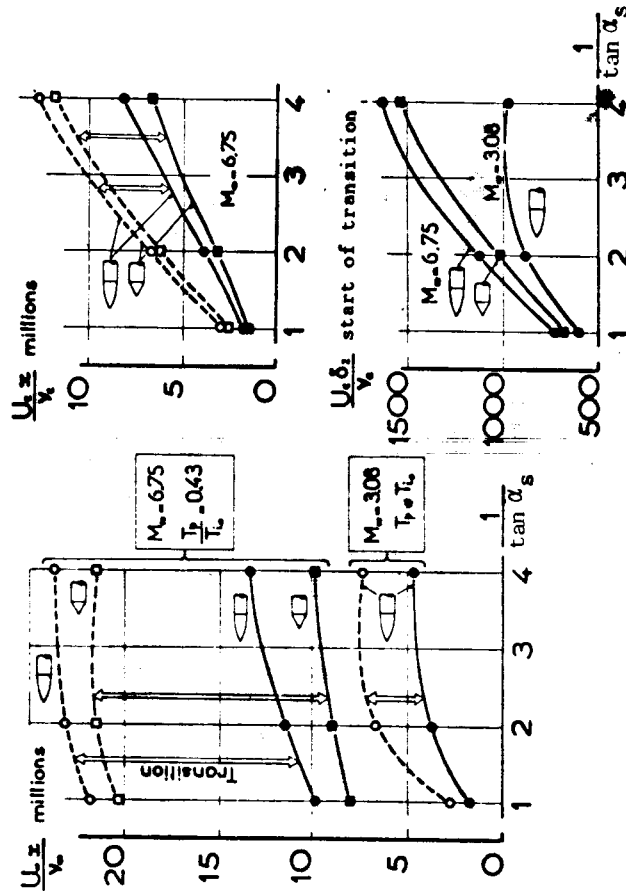


Fig.9 Transition Reynolds Numbers.

Translated for the National Aeronautics and Space Administration by the O.W. Leibiger Research Laboratories, Inc.